International Journal of Materials Science and Applications
2025, Vol. 14, No. 2, pp. 53-59
https://doi.org/10.11648/j.ijmsa.20251402.12

Research Article

First Principles Assessment of Electronic and Magnetic Properties of Fe and Ni Doped ZnO for Spintronic Applications

Ahmed Bappah Abdullahi[1], Nasiru Aabdullahi Lawan[2], Mansur Said[3, *], Garba Babaji[2], Yahaya Aliyu Danmaraya[4]

[1]Department of Physics, Faculty of Science, Gombe State University, Gombe, Nigeria
[2]Department of Physics, Faculty of Physical Sciences, Bayero University, Kano, Nigeria
[3]Department of Physics, Faculty of Science, Yusuf Maitama Sule University, Kano, Nigeria
[4]Department of Chemistry, Faculty of Science, Yusuf Maitama Sule University, Kano, Nigeria

Abstract

Presence of room temperature ferromagnetism (RTFM) is essential for the generation of new class of materials that have magnetic as well as semiconducting properties known as diluted magnetic semiconductors (DMSs). A 3d Transition metals (TMs) doping on DMSs improve their electrical, thermal and magnetic properties and also enhance their potentiality for the generation of emerging spintronic devices. Electronic and magnetic behaviors of, Fe and Ni doped ZnO were investigated using the density functional theory (DFT) with generalized gradient approximation and Hubbard on-site corrections (GGA+U). The results illustrated that pure and doped systems of ZnO have a direct bandgap. The calculated bandgap of pure ZnO is in agreement with the experimental findings while a decrease in bandgap found is due to the doping of Fe and Ni on ZnO, respectively. Total density of state (TDOS) plot illustrates that pure ZnO is diamagnetic, while Ferromagnetism was observed due to doping effect of Fe and Ni on ZnO. Results from Partial density of states (PDOS) shows that the asymmetric behavior of spin up and spin down on the d-electrons of Fe on ZnO are more compared to that of Ni on ZnO. Making it more promising candidate for spintronic applications.

Keywords

DMSs, RTFM, TMs, ZnO, DFT

1. Introduction

In view of their possible application in spintronic devices, Diluted Magnetic Semiconducting (DMS) materials have been receiving a lot of attention due to their capability to utilize both electrons charge and spin degree of freedom [1]. DMSs exhibit both magnetic and semiconducting behavior for the generation of new class of materials. These materials have ferromagnetic as well as semiconducting properties that make them promising candidates for the vast applications in

*Corresponding author: mansursaid79@gmail.com (Mansur Said)

Received: 2 February 2025; **Accepted:** 17 February 2025; **Published:** 29 May 2025

logic devices, spin valve transistors, diodes, non-volatile storage, ultra-fast optical switches and quantum computing devices [2-4]. Low Curie temperature T_c nature of most DMSs tends to limits their potentiality to offer the aforementioned applications at room temperature. Previous experimental and theoretical approaches have demonstrated that room temperature ferromagnetism (RTFM) may be detected when DMSs are doped with transition metals (TMs). Although the exact origin of RTFM is still a matter of debate, it is widely regarded that RTFM is mainly due to defects induced like vacancies, substitutions or interstitial [5-7]. The induced defects modify the material's electrical, thermal, and magnetic characteristics. The FM can be observed by hosting the magnetic ions of the TM into metallic ions of the parent diluted magnetic semiconductor making it possible for spintronic devices to function at ambient situations [8].

ZnO as diluted magnetic semiconductor has attracted attention [9], due to its direct bandgap of (3.4eV), low in cost, large exciting binding energy (60eV), non-toxic nature, strong cohesive energy and good thermal stability make it a promising applicant [10-18]. These exceptional properties of ZnO based DMS is used in solar cells, transducer, luminent materials, heat mirrors, semiconductor heterojunctions, thin film transistors, gas sensors, transparent conductor, biomedical when doped with 3d TMs like Fe, Co, Ni, Mn, etc [15, 19, 20]. Among those TMs, Fe and Ni possess exceptional magnetic properties and have atomics numbers and metallic radii Fe(Z=26,r(Å)=0.76Å), Ni (Z=28,r(Å)=0.68Å) which is very close to that of Zinc (Z=30,r(Å)=0.74Å), making them excellent candidates for the doping process [4].

A microwave-based synthesis technique was utilized to investigate the magnetic characteristics of Iron and Nickel dope with ZnO nanoparticles. The pure and Iron doped ZnO nanoparticles formed a single layer Wurtzite hexagonal-shaped crystal structure without any impurities, but Nickel doped ZnO nanoparticles formed NiO impurities. The magnetic studies indicated a diamagnetic behavior for the pure ZnO. Meanwhile, both Iron and Nickel doped ZnO showed clear room temperature ferromagnetism [6]. [3] The energy gap and defect-engineered optical and magnetic behaviors of ZnO-based diluted magnetic semiconducting nanoparticles have been studied using the co-precipitation technique.

The influence of Ni doping on the optical, structural, and morphological features of ZnO thin films produced by Metal-Organic Solution Immersion Liquid Assisted Reaction (MSILAR) was investigated using experimental and DFT methods. The result revealed a reduction in bandgap from 3.23eV to 3.11eV. The first principle computation was employed to demonstrate the influence of Ni on the electrical and magnetic behaviors. It revealed that ZnO and Ni doped ZnO is a direct bandgap semiconductor, and Ni-3d electrons are the principal source of magnetic dipole moment in ZnO matrix. With recent advancements in computing software, first-principles (DFT) has emerged as an affordable and simple approach for studying the behavior of TMs doped ZnO. The goal of this study is to explore the electronic and magnetic properties of pure ZnO, Fe, and Ni doped ZnO for spintronic applications using density functional theory (DFT) employing the generalized gradient approximation with Hubbard-like on-site correction (GGA+U). The computation was performed using the Quantum Espresso package.

2. Theoretical Background

First principles in physics, chemistry, and material science are an investigative method used to study material properties at the atomic and molecular levels. This technique employs computations based on quantum mechanics, particularly the Schrödinger equation, to analyze unit cell structures, as well as the optical and electronic properties of materials [21].

$$\hat{H}\Psi = E\Psi \tag{1}$$

The Hamiltonian operator ($\hat{H}$) represents the total energy of a system, including kinetic and potential energies from the Coulombic interactions between electrons and nuclei. The wavefunction (Ψ) describes the system, and E denotes its energy.

$$\hat{H} = \sum_{I=1}^{N} \frac{P_I^2}{2M_1} + \sum_{i=1}^{n} \frac{P_i^2}{2m_1} + \sum_{i\neq j} \frac{e^2}{|r_i - r_j|} + \sum_{I\neq j} \frac{Z_I Z_J e^2}{|R_I - R_J|} - \sum_{ij} \frac{Z_1 e^2}{|R_I - r_i|} \tag{2}$$

Density Functional Theory (DFT) is a computational quantum mechanical method used to study the electronic structure of atoms, molecules, and condensed phases. Developed by Hohenberg and Kohn, DFT states that all ground-state properties of many-particle systems are determined by electron density. In 1965, Kohn and Sham reformulated the problem, making DFT practical for real-world applications [22].

$$\rho(r) = \Psi^2(r) \tag{3}$$

The Kohn-Sham method introduced a framework that approximates the real many-electron system by generating independent particle equations, which can be solved numerically. This approach allows for the calculation of the system's total energy [23].

$$E_v[\rho] = \int \rho(r)v(r)dr + \overline{T}_s[\rho] + \frac{1}{2}\iint \frac{\rho(r_1)\rho(r_2)}{r_{12}} dr_1 dr_2 + E_{xc}[\rho] \tag{4}$$

The exchange-correlation energy Exc in DFT includes exchange energy, correlation energy, Coulombic correlation energy, and self-interaction correction. Since no exact formulation exists for the XC potential, approximations are used to ensure the accuracy of DFT computations.

The Kohn-Sham equations lack analytical solutions, requiring further approximations like the local density approximation (LDA) and generalized gradient approximation (GGA). However, LDA and GGA tend to underestimate band gaps by 50-100% due to over-delocalization of valence electrons and over-stabilization of metallic ground states [24] To overcome these limitations, an orbital-dependent on-site Coulomb repulsion term, Hubbard U, is added to the XC term, leading to the LDA+U or GGA+U methods [25].

$$E_{LDA+U}[n(r)] = E_{LDA}[n(r)] + E_U[n(r)] - E_{dc} \quad (5)$$

In this context, $n(r)$ represents the electron density probability, E_{LDA} is the energy from the traditional LDA functional, $E_U$is the Hubbard energy, and E_{dc} accounts for the double-counting correction energy.

Kohn-Sham (KS) band gaps are not exact experimental band gaps due to physical limitations, though the KS band structure often closely resembles the true band structure. The band dispersion aligns well with experimental results. The semiconductor band gap (Eg) is defined as the energy difference between the ground-state energies of N and N±1 particle systems [26].

$$E_g = E(N+1) + E(N-1) - 2E(N) = I - A \quad (6)$$

Here, A represents the electron affinity and I ionization energy of the systems respectively. Principally, the energy of the lowest conduction band is given by $E_c = E_{N+1} - E_N$ and that of the valance band as $E_V = E_N - E_{N-1}$.

The density of electronic states $g(E)$ represents the number of allowed electron energy states per unit energy interval around a specific energy E, including spin degeneracy. It influences key properties of crystals, particularly semiconductors, such as optical, thermodynamic, and transport characteristics [27]. The density of states $g(E)$ can be expressed as;

$g(E)$ = 2×(number of states which have an energy E ($\vec{K}$) equal to E)

Which can be represents mathematically as;

$$g(E) = 2\sum_{\vec{K}} \delta|E(\vec{K}) - E| \quad (7)$$

The wave vector $\vec{K}$ is used to index the permissible electron states, so the summing applies to all values. The Dirac function $\delta(x)$ is a particular even function.

3. Computational Method

Two Zinc and two Oxygen formed the unit cell of the wurtzite structure of ZnO. A $2 \times 2 \times 2$ supercell of ZnO is formed by stacking-eight unit cells of the wurtzite ZnO structure together. The supercell has 32 atoms, 16 Zinc and 16 oxygen, as seen in Figure 1. The structure and input files were built using BURAI (GUI) version 1.3.1. The electronic and magnetic properties of ZnO system were investigated using density functional theory (DFT) with the generalized gradient approximation and a Hubbard-like on-site correction (GGA+U). Rappe Rabe Kaxiras Joanno-poulos' (rrkjus) ultrasoft pseudopotential was utilized to depict electron-ion interaction. This was due to the advantage of it on TM and also on energy gap. The doping was carried out on the Zn atom which was either been replaced by two Fe or two Ni atoms and which account for 6.2% atomic concentration and this was done due to the computational power available. A K-mesh of $4 \times 4 \times 2$ and 1350eV energy cut-off were set for the undoped and doped system of ZnO. The Hubbard parameter of U(Zn)=10eV, U(O)= 7eV, U(Fe)= 5.4eV, U(Ni)= 6.4eV were taken from previous research. The computations were done with the quantum espresso simulation package.

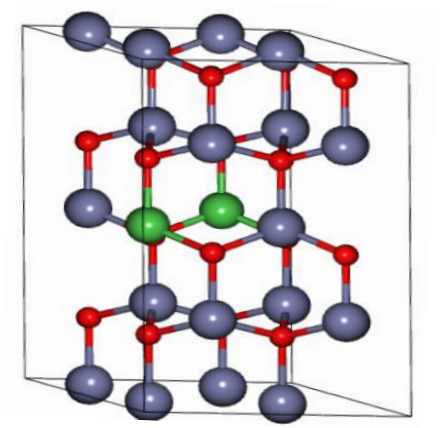

Figure 1. *2x2x2 wurzite ZnO, the green color represents the doping site of either Fe or Ni.*

4. Results and Discussion

The result of Figure 2 (a). illustrates the computed band structure of pure ZnO. The valence band maximum (VBM) and conduction band minimum (CBM) align at the center of the Brillion Zone, proving that pure ZnO is a direct gap semiconductor. And this shows that the material can be good for light emission, high optical absorption and compact efficient material. Also it indicates that with lower power induce a higher efficient material can be produce. The computed bandgap energy of 3.38eV is reported, is in agreement with the experimental band gap (3.40eV), which is typically undervalued by LDA or GGA functional. With doping of Fe and Ni doped ZnO, it was observed that there was decrease in in the energy gap of about 0.93eV and 0.51eV from that of the pure ZnO respectively as shown in Figures 3 and 5. The bandgap energies found are 2.45eV and 2.87eV for Fe and Ni doped ZnO respectively. The results also indicated that Fe and Ni doped ZnO are direct bandgap semiconductors.

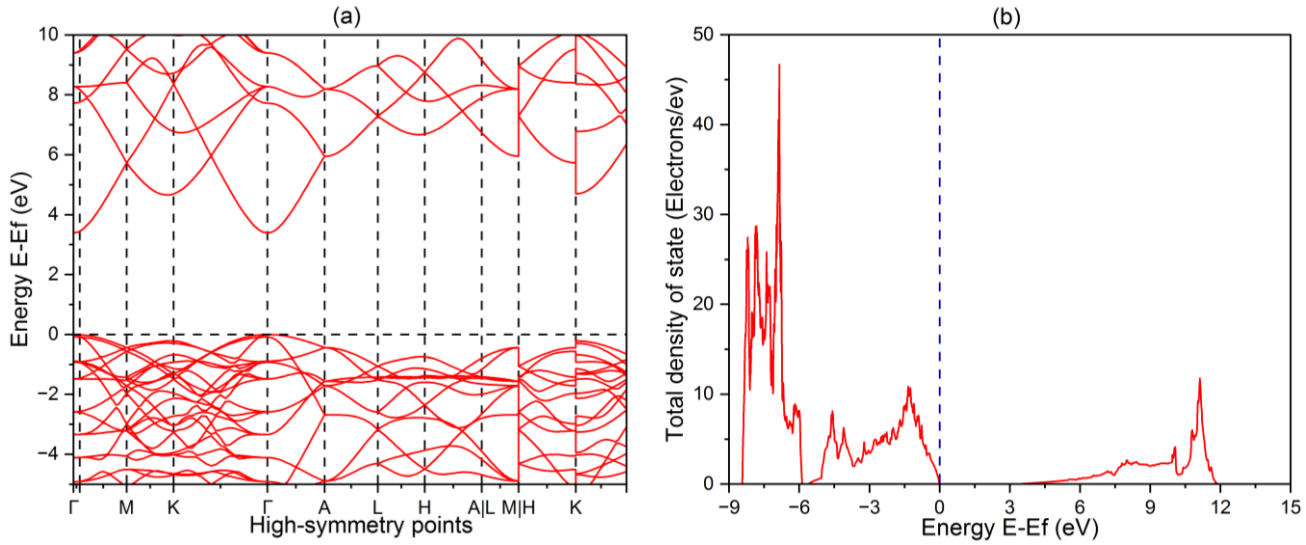

Figure 2. *(a). Electronic band structure of pure ZnO. The horizontal dotted line represent the Fermi energy (b) Total density of state (TDOS) of pure ZnO. The Vertical blue dotted line is the Fermi energy.*

Figure 2 (b) presents the total density of state of the pure ZnO. The valence band lies between -8.43eV and 0eV, whereas the conduction band is between 3.88eV and 11.80eV, proving the semiconducting nature of pure ZnO. The Fermi energy which is the reference energy, was specified as zero. The spin up and down electronic states were superimposed, and the net magnetic dipole moment per cell calculated is $0\mu_B$ see Figure 2. This confirmed the non-magnetic nature of pure ZnO. Figures 4(a) and 6(a) illustrate the total spin density of state (TDOS) for both Fe-doped ZnO and Ni-doped ZnO and It was found that, unlike pure ZnO, the total density of state (TDOS) of spin up and spin down is asymmetrical, owing to broken degeneracy states. The asymmetry implies that Fe and Ni doped ZnO are ferromagnetic. Fe doped ZnO had a total magnetic moment of $4.03\mu_B$ per cell, while Ni doped ZnO had a magnetic moment of $2.0\mu_B$. This suggests that both Fe and Ni doped ZnO exhibit ferromagnetism.

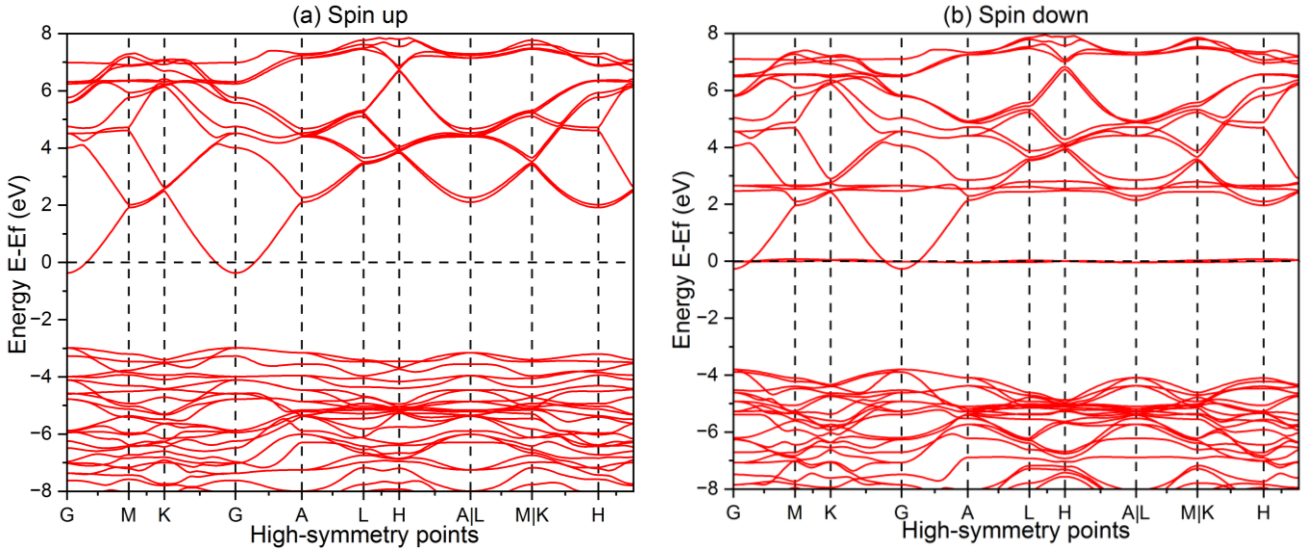

Figure 3. *Electronic band structure of Fe: ZnO (a) Spin up (b) Spin down. The horizontal dot line represents the Fermi energy.*

The partial density of states was used to study the root of ferromagnetism in Fe and Ni doped ZnO. Figure 4 (b). Shows the PDOS of Fe-doped ZnO. The valance band is mainly occupied by O-2p, with little contributions of Zn-4s and Fe-3d electron states, whereas the conduction band is largely occupied with spin-down Fe-3d and orbitals intermixing between Zn-4s and O-2p electron states. Zn-4s and O-2p have the equal number of spin up and spin down states, but Fe-3d had

asymmetrical spin up and spin down states, indicating that the ferromagnetic behavior in Fe doped ZnO is primarily due to Fe-3d electrons. Similar scenario can be observed for Ni doped ZnO in Figure 6 (b) however the influence of Ni-3d spin down electron state in the conduction band is small compared to that of Fe-3d. This implied that Fe doped ZnO is more ferromagnetic than Ni doped ZnO.

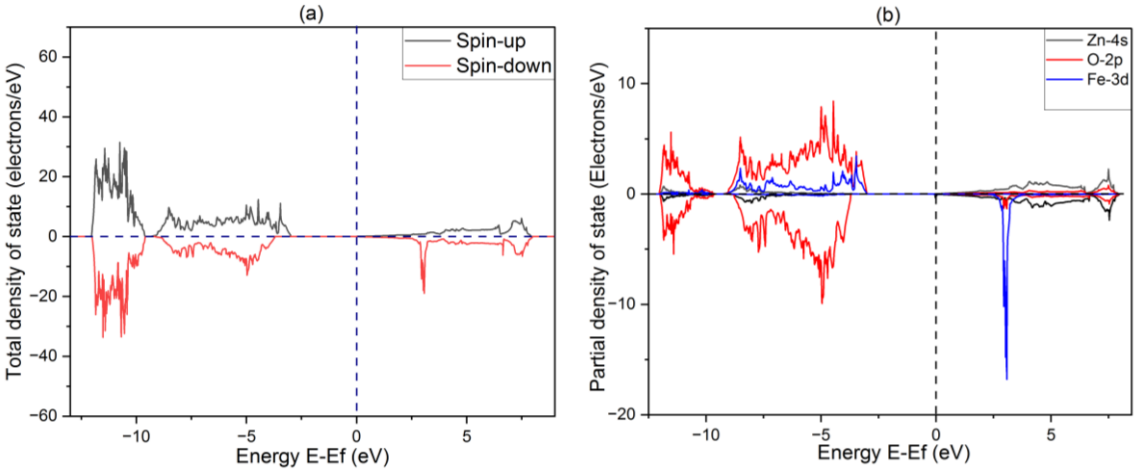

Figure 4. *(a) Total density of states (TDOS) of Fe:ZnO (b) Partial density of states (PDOS) of Fe:ZnO.*

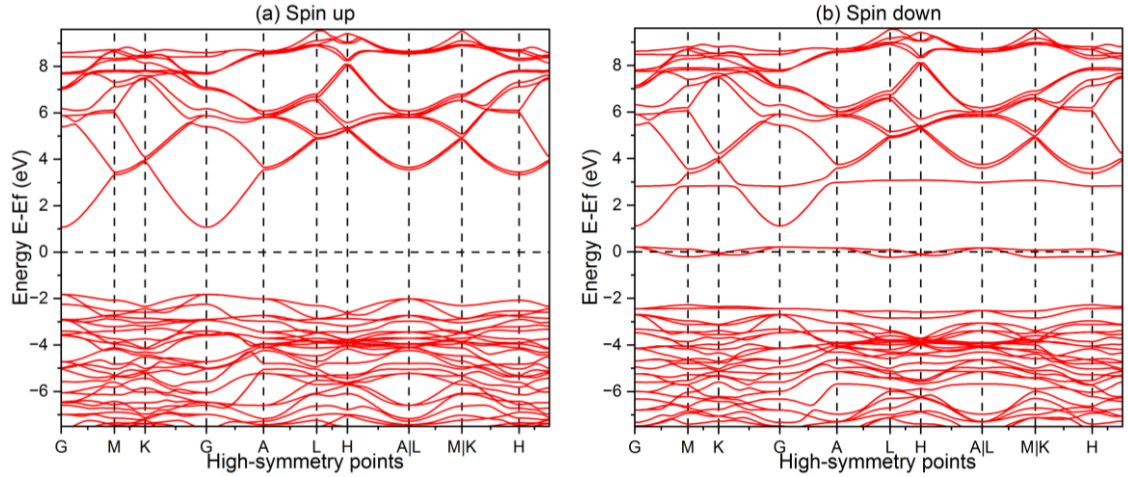

Figure 5. *Electronic band structure of Ni:ZnO (a) Spin up (b) Spin down.*

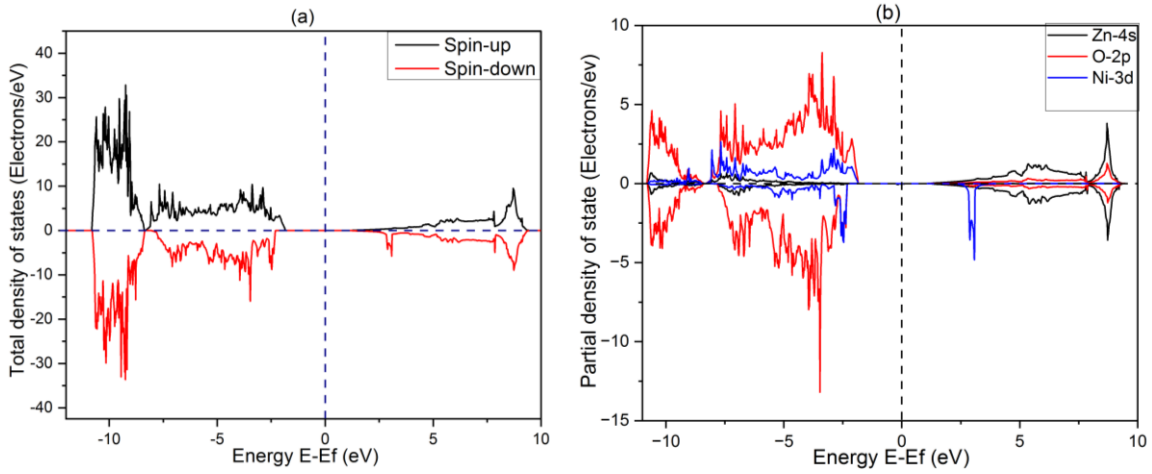

Figure 6. *(a) Total density of state (TDOS) of Ni:ZnO (b) Partial density of states (PDOS) of Ni:ZnO.*

5. Conclusion

The Electronic and magnetic properties of pure, Fe and Ni doped ZnO have been studied using the density functional theory (DFT) with GGA+U. The results shown that pure ZnO and doped systems of ZnO are direct bandgap semiconductor. The bandgap of pure ZnO was calculated and is in good agreement with the experimental results while a decrease in bandgap was recorded for both Fe and Ni doped ZnO respectively. Total density of state (TDOS) result showed that pure ZnO exhibit a diamagnetic behavior while both Fe and Ni doped ZnO exhibited ferromagnetic behavior due to asymmetric change of spin up and spin down electrons states. According to partial density of state (PDOS), the conduction band is dominated by spin-down Fe-3d and Ni-3d, also by the orbital intermixing of Zn-4s and O-2p electrons states. Meaning that both Fe and Ni doped ZnO are ferromagnetic, but the contributions of Fe-3d spin down electrons are much when compared to that of Ni-3d. This makes Fe doped ZnO more Ferromagnetic and more promising for spintronic applications.

Abbreviations

RTFM	Room Temperature Ferromagnetism
DMS	Diluted Magnetic Semiconductors
TMs	Transition Metals
DFT	Density Functional Theory
ZnO	Zinc Oxide
GGA	Generalize Gredient Approximation
GGA+U	Generalized Gredient Approximation + Hubbard Corrections
PDOS	Partial Density of State
TDOS	Total Density of State
Fe	Iron
Ni	Nickel
Mn	Manganese
NiO	Nickel Oxide
H	Hamiltonian
LDA	Local Density Approximation
KS	Khon Sham
GUI	Graphical User Interface
VBM	Valence Band Maximum
CBM	Conduction Band Minimum

Conflicts of Interest

The authors declare no conflict of interest regarding the publication of this work.

References

[1] I. Jabbar *et al.*, "Diluted magnetic semiconductor properties in TM doped ZnO nanoparticles," *RSC Adv.*, vol. 12, no. 21, pp. 13456–13463, Apr. 2022, https://doi.org/10.1039/D2RA01210C

[2] Z. H. Alhashem, "Ni-doped ZnO nanoparticles derived by the sol – gel method : structural, optical, and magnetic characteristics," *Arab. J. Chem.*, vol. 17, no. 5, p. 105701, 2024, https://doi.org/10.1016/j.arabjc.2024.105701

[3] F. Kabir, A. Murtaza, W. ur Rehman, A. Ghani, and S. Yang, "Energy gap and defects engineered optical, and magnetic properties of ZnO-based diluted magnetic semiconducting nanoparticles," *Results Phys.*, vol. 60, no. September 2023, p. 107650, 2024, https://doi.org/10.1016/j.rinp.2024.107650

[4] I. Benaicha, J. Mhalla, A. Raidou, A. Qachaou, and M. Fahoume, "Effect of Ni doping on optical, structural, and morphological properties of ZnO thin films synthesized by MSILAR: Experimental and DFT study," *Materialia*, vol. 15, Mar. 2021, https://doi.org/10.1016/j.mtla.2021.101015

[5] A. Sedky, A. Mossad, M. A. Sayed, and A. Almohammedi, "Results in Physics On the dielectric and magnetic properties of Al doped Pr : 123 for advanced devices : A comparison with ZnO," *Results Phys.*, vol. 52, no. July, p. 106834, 2023, https://doi.org/10.1016/j.rinp.2023.106834

[6] S. Said Abdullahi, G. Shehu Musa Galadanci, N. Mohd Saiden, and J. Ying Chyi Liew, "Assessment of Magnetic Properties between Fe and Ni Doped ZnO Nanoparticles Synthesized by Microwave Assisted Synthesis Method Malaysia a," 2021. [Online]. Available: www.scientific.net

[7] G. Akgul and F. Aksoy, "Impact of cobalt doping on structural and magnetic properties of zinc oxide nanocomposites synthesized by mechanical ball-milling method," *Colloid Interface Sci. Commun.*, vol. 48, no. June 2021, p. 100611, 2022, https://doi.org/10.1016/j.colcom.2022.100611

[8] S. S. Abdullahi, G. Shehu, M. Galadanci, N. M. Saiden, J. Ying, and C. Liew, "Assessment of Magnetic Properties between Fe and Ni Doped ZnO Nanoparticles Synthesized by Microwave Assisted Synthesis Method," vol. 317, pp. 119–124, 2021.

[9] J. Arul Mary, J. Judith Vijaya, M. Bououdina, L. John Kennedy, J. H. Daie, and Y. Song, "Investigation of structural, surface morphological, optical properties and first-principles study on electronic and magnetic properties of (Ce, Fe)-co doped ZnO," *Phys. B Condens. Matter*, vol. 456, pp. 344–354, 2015, https://doi.org/10.1016/j.physb.2014.09.023

[10] P. Sikam, P. Moontragoon, J. Jumpatam, S. Pinitsoontorn, P. Thongbai, and T. Kamwanna, "Structural, Optical, Electronic and Magnetic Properties of Fe-Doped ZnO Nanoparticles Synthesized by Combustion Method and First-Principle Calculation," *J. Supercond. Nov. Magn.*, vol. 29, no. 12, pp. 3155–3166, 2016, https://doi.org/10.1007/s10948-016-3690-0

[11] H. Cao *et al.*, "First-principles study on electronic and magnetic properties of (Mn,Fe)-codoped ZnO," *J. Magn. Magn. Mater.*, vol. 352, no. 1, pp. 66–71, 2014, https://doi.org/10.1016/j.jmmm.2013.10.008

[12] M. Sk, S. S. Shastri, and S. K. Pandey, "DFT study of 3d transition metal-doping effect in wurtzite-ZnO for photovoltaic applications," vol. 030478, no. July, 2019, https://doi.org/10.1063/1.5113317

[13] E. K. Droepenu, "Zinc Oxide Nanoparticles Synthesis Methods and its Effect on Morphology : A Review," vol. 12, no. 3, pp. 4261–4292, 2022.

[14] P. Kaur, S. Chalotra, H. Kaur, A. Kandasami, and D. Paul, "Applied Surface Science Advances Role of Bound Magnetic Polaron Model in Sm Doped ZnO : Evidence from Magnetic and Electronic Structures," *Appl. Surf. Sci. Adv.*, vol. 5, no. April, p. 100100, 2021, https://doi.org/10.1016/j.apsadv.2021.100100

[15] Z. Gou, H. Yang, and P. Yang, "Investigation on electronic and magnetic properties of (Fe, In) co-doped ZnO," *J. Alloys Compd.*, vol. 695, pp. 1378–1382, 2017, https://doi.org/10.1016/j.jallcom.2016.10.279

[16] S. Aslanzadeh, "Transition metal doped ZnO nanoclusters for carbon monoxide detection: DFT studies," *J. Mol. Model.*, vol. 22, no. 7, 2016, https://doi.org/10.1007/s00894-016-3032-y

[17] B. Ul Haq, R. Ahmed, A. Shaari, N. Ali, Y. Al-Douri, and A. H. Reshak, "Comparative study of Fe doped ZnO based diluted and condensed magnetic semiconductors in wurtzite and zinc-blende structures by first-principles calculations," *Mater. Sci. Semicond. Process.*, vol. 43, pp. 123–128, 2016, https://doi.org/10.1016/j.mssp.2015.12.010

[18] C. Soumya and P. P. Pradyumnan, "Synthesis and characterizations of nickel doped zinc oxide," in *AIP Conference Proceedings*, Nov. 2020, vol. 2287, https://doi.org/10.1063/5.0029876

[19] D. Guruvammal, S. Selvaraj, and S. Meenakshi Sundar, "Structural, optical and magnetic properties of Co doped ZnO DMS nanoparticles by microwave irradiation method," *J. Magn. Magn. Mater.*, vol. 452, pp. 335–342, 2018, https://doi.org/10.1016/j.jmmm.2017.12.097

[20] P. L. Hadimani, S. S. Ghosh, and A. Sil, "Preparation of Fe doped ZnO thin films and their structural, magnetic, electrical characterization," *Superlattices Microstruct.*, vol. 120, pp. 199–208, 2018, https://doi.org/10.1016/j.spmi.2018.05.029

[21] K. Harun, N. A. Salleh, B. Deghfel, M. K. Yaakob, and A. A. Mohamad, "DFT + U calculations for electronic, structural, and optical properties of ZnO wurtzite structure: A review," *Results Phys.*, vol. 16, no. September 2019, p. 102829, 2020, https://doi.org/10.1016/j.rinp.2019.102829

[22] R. A. Ismail, A. B. Suleiman, A. S. Gidado, A. Lawan, and A. Musa, "Investigation of the Effects of Solvents on the Structural, Electronic and Thermodynamic Properties of Rosiglitazone Based on Density Functional Theory," *Phys. Sci. Int. J.*, no. May, pp. 1–18, 2019, https://doi.org/10.9734/psij/2019/v21i230103

[23] A. S. Gidado, S. Kulsoom, A. Musa, and U. M. Ibrahim, "Determination of the Electronic Structure, Charge-transfer, and Optical Properties of Neutral, Anionic, and Cationic Perfluoropentacene," vol. 33, no. 4, pp. 54–68, 2024.

[24] "A QUANTUM ESPRESSO STUDY OF NITROGEN DOPED GRAPHENE USING," vol. 5, no. 3, pp. 100–107, 2022.

[25] M. Cococcioni, *The LDA+U Approach: A Simple Hubbard Correction for Correlated Ground States*, vol. 2. 2012.

[26] H. Dixit, "First-principles electronic structure calculations of transparent conducting oxide materials," *Cmt.Ua.Ac.Be*, 2012, [Online]. Available: http://www.cmt.ua.ac.be/ua/HemantDixit.pdf

[27] M. S. Ummah, No. Covariance structure analysis on health-related indicators in home-bound elderly with a focus on subjective sense of healthTitle, vol. 11, no. 1. 2019.